Systematic Review and Meta-Analysis

Medicine

OPEN

Application of network pharmacology and molecular docking approach to explore active compounds and potential pharmacological mechanisms of *Aconiti Lateralis Radix Praeparata* and *Lepidii Semen Descurainiae Semen* for treatment of heart failure

Meng-Qi Yang, PhD[a], Cong Chen, PhD[b], Yi-Fei Mao, PhD[b], Yan Li, PhD[d], Xia Zhong, PhD[a], Yi-Ding Yu, MD[c], Yi-Tao Xue, PhD[d,*], Yong-Mei Song, PhD[b]

Abstract

Background: Heart failure (HF) is the end stage of the development of heart disease, whose prognosis is poor. The previous research of our team indicated that the formulae containing *Aconiti Lateralis Radix Praeparata* and *Lepidii Semen Descurainiae Semen* (ALRP-LSDS) could inhibit myocardial hypertrophy, inhibit cardiomyocyte apoptosis, delay myocardial remodeling (REM), and improve the prognosis of patients with HF effectively. In order to explore the mechanism of ALRP-LSDS for the treatment of HF, a combined approach of network pharmacology and molecular docking was conducted.

Methods: Public database TCMSP was used to screen the active compounds of ALRP-LSDS. The targets of screened active compounds were obtained from the TCMSP database and predicted using the online analysis tool PharmMapper. The targets of HF were obtained from 6 databases including GeneCards, OMIM, DrugBank, TTD, PharmGKB, and DisGeNET. Protein–protein interaction and enrichment analysis were performed, respectively, by STRING and Metascape online tools after merging the targets of active compounds and HF. Cytoscape software was used to conduct networks. Finally, molecular docking was performed by Vina to verify the correlation between key targets and active compounds.

Results: Final results indicated that the active compounds including β-sitosterol, isorhamnetin, quercetin, kaempferol, and (*R*)-norcoclaurine, the targets including AKT1, CASP3, and MAPK1 might be the main active compounds and key targets of ALRP-LSDS for the treatment of HF separately. The binding ability of AKT1 to the main active compounds was better compared with the other 2 key targets, which means it might be more critical. The pathways including AGE-RAGE signaling pathway in diabetic complications, Pathways in cancer, and Fluid shear stress and atherosclerosis might play important roles in the treatment of HF with ALRP-LSDS. In general, ALRP-LSDS could inhibit cardiomyocyte apoptosis, delay REM, and improve cardiac function through multicompound, multitarget, and multipathway, which contributes to the treatment of HF.

Conclusions: Based on the combined approach of network pharmacology and molecular docking, this study screened out the main active compounds, key targets, and main pathways of ALRP-LSDS for the treatment of HF, and revealed its potential mechanisms, providing a theoretical basis for further research.

This work is financially supported by the grant of National Nature Science Foundation of China (81774247).

The authors declare that they have no conflicts of interest.

The datasets generated during and/or analyzed during the current study are available from the corresponding author on reasonable request.

Supplemental digital content is available for this article.

[a] First School of Clinical Medicine, Shandong University of Traditional Chinese Medicine, Jinan, China, [b] Institute for Literature and Culture of Chinese Medicine, Shandong University of Traditional Chinese Medicine, Jinan, China, [c] College for Traditional Chinese Medicine, Shandong University of Traditional Chinese Medicine, Jinan, China, [d] Department of Cardiology, The Affiliated Hospital of Shandong University of Traditional Chinese Medicine, Jinan, China.

**Correspondence: Yi-Tao Xue, Department of Cardiology, The Affiliated Hospital of Shandong University of Traditional Chinese Medicine, Jinan 250024, China (e-mail: xytsdzydfy@126.com).*

Copyright © 2022 the Author(s). Published by Wolters Kluwer Health, Inc. This is an open-access article distributed under the terms of the Creative Commons Attribution-Non Commercial License 4.0 (CCBY-NC), where it is permissible to download, share, remix, transform, and buildup the work provided it is properly cited. The work cannot be used commercially without permission from the journal.

How to cite this article: Yang M-Q, Chen C, Mao Y-F, Li Y, Zhong X, Yu Y-D, Xue Y-T, Song Y-M. Application of network pharmacology and molecular docking approach to explore active compounds and potential pharmacological mechanisms of Aconiti Lateralis Radix Praeparata and Lepidii Semen Descurainiae Semen for treatment of heart failure. Medicine 2022;101:33(e30102).

Received: 6 December 2021 / Received in final form: 15 June 2022 / Accepted: 30 June 2022

http://dx.doi.org/10.1097/MD.0000000000030102

Abbreviations: ACEI = angiotensin-converting enzyme inhibitors, ADME = absorption, distribution, metabolism and excretion, AGE/AGEs = advanced glycation end products, AKT1/PKB = RAC-alpha serine/threonine protein kinase, protein kinase B, ALRP = *Aconiti Lateralis Radix Praeparata*, Bcl-2 = B-cell lymphoma-2, Bcl-XL = B-cell lymphoma extra large, BP = biological processes, Caspase-3 = Cysteiny aspartate-specific proteinase-3, Caspase-6 = Cysteiny aspartate-specific proteinase-6, Caspase-7 = Cysteiny aspartate-specific proteinase-7, CC = cell components, DL = drug-likeness, EC = endothelial cell, GO = Gene Ontology, GSK-3β = glycogen synthase kinase-3β, HF = heart failure, IL1 = interleukin-1, IL6 = interleukin-6, JAK = Janus Kinase, KEGG = Kyoto Encyclopedia of Genes and Genomes, LSDS = *Lepidii Semen Descurainiae Semen*, MAPK1/ERK2 = mitogen-activated protein kinase 1, extracellular signal-regulated kinase 2, MAPKs = mitogen-activated protein kinases, MEK = mitogen-activated protein kinase kinase, MF = molecular functions, mPTP = mitochondrial permeability transition pore, NADPH = nicotinamide adenine dinucleotide phosphate, NF-κB = nuclear factor kappa B, OB = oral bioavailability, OMIM = Online Mendelian Inheritance in Man, PI3K = phosphatidylinositol 3-kinase, PKC = protein kinase C, PPI = protein–protein interaction, Raf = RAF proto-oncogene serine/threonine protein kinase, RAGE = receptor for advanced glycation end products, RCSB PDB = Research Collaboratory for Structural Bioinformatics protein data bank, REM = myocardial remodeling, SGLT-2i = sodium glucose cotransporter 2 inhibitors, STAT = signal transducer and activator of transcription, TCM = Traditional Chinese Medicine, TCMSP = Traditional Chinese Medicine Systems Pharmacology, TNF-α = tumor necrosis factor-α, TTD = therapeutic target database, VEGF = vascular endothelial growth factor.

Keywords: *Aconiti Lateralis Radix Praeparata*, heart failure, *Lepidii Semen Descurainiae Semen*, molecular docking, network pharmacology

1. Introduction

Heart failure (HF) is a complex clinical syndrome characterized by a series of symptoms and signs caused by structural or functional cardiac abnormalities, which is the common outcome of various end-stage cardiovascular diseases. It is a leading and increasing cause of morbidity and mortality worldwide, despite the efficacy of many therapies for patients with HF.[1]

The occurrence and development of HF is a series of processes of myocardial pressure or volume overload, which leads to compensatory myocardium hypertrophy, and then decompensation, which leads to myocardial injury. REM is the basic mechanism of its occurrence and development. Pressure and volume overload will trigger the remodeling cascade, a process that initially protects the heart as a compensatory mechanism, but over time becomes decommissioned, leading to enlarged heart, decreased heart function, and ultimately HF.[2,3] Many large clinical trials have demonstrated that angiotensin-converting enzyme inhibitors (ACEI), β-blockers, aldosterone, and other neuroendocrine inhibitors can change the biological properties of failing myocardium, delay or even reverse REM, improve the prognosis and reduce the mortality of patients with HF.[4] Therefore, the treatment mode mainly aimed at improving neuroendocrine abnormalities and preventing REM should be the direction of our future research.

Traditional Chinese medicine (TCM) herbs ALRP and LSDS are both commonly used in the treatment of HF. A study has analyzed the TCM prescriptions for HF in recent 20 years, and the results show that both ALRP and LSDS are the most frequently used drugs for HF.[5] TCM Qiliqiangxin Capsule, the Fuxin mixture (*Aconiti Lateralis Radix Praeparata*, *Lepidii Semen Descurainiae Semen*, *Epimrdii Herba*, *Angelicae Sinensis Radix*, *Alisma Orientale* (*Sam.*) *Juz.*, *Phellodendri Chinrnsis Cortex*) and Fuxin decoction (*Aconiti Lateralis Radix Praeparata*, *Lepidii Semen Descurainiae Semen*, *Hedysarum Multijugum Maxim.*) summarized by Prof. Xue for the treatment of HF all contain ALRP-LSDS. Experimental studies have revealed that Qiliqiangxin capsule can inhibit myocardial hypertrophy, REM and improve cardiac function in mice with pressure overload effectively. Meanwhile, evidence-based medical research QL-BACD test also confirms that Qiliqiangxin capsule can improve the quality of life and prognosis of patients with HF.[6] Our previous experiments also showed that Fuxin mixture could effectively inhibit myocardial hypertrophy and cardiomyocyte apoptosis and delay REM through the regulation of the c-Raf/MEK/ERK pathway,[7] PI3K/Akt/GSK-3β pathway[8] and β1/AR/cAMP/PKA pathway.[9] Fuxin decoction can also improve the energy metabolism of myocardial mitochondria and myocardial apoptosis by improving the permeability of mPTP,[10] improving the prognosis of patients with HF. In the heart, an organ with high energy demand, cardiac energy metabolism, and mitochondrial function, structural disorders are closely related to HF. Mitochondrial dysfunction leads to impaired myocardial energy and increased oxidative stress in HF, while the opening of mPTP triggers cell death and myocardial remodeling, promoting the process of HF.[11] However, no directly experimental studies have been conducted to explore the role of ALRP-LSDS in the treatment of HF and its potential mechanism. Therefore, it is significant to explore the active compounds and potential mechanism of ALRP-LSDS in the treatment of HF.

A combined approach of network pharmacology and molecular docking, which has been widely used in the study of the mechanism of TCM in recent years, was used to explore the potential mechanism of ALRP-LSDS in the treatment of HF. Network pharmacology can deepen our understanding of the active compounds of TCM through the interaction network of "multigene, multitarget, and multipathway" and provide strong evidence for the biological targets and potential mechanisms of action of TCM in treating various diseases.[12,13] Based on the docking mode of "multi-target-single-ligand," molecular docking enables the small molecule to be identified with biomacromolecules to form molecular complexes according to space and energy matching, further clarifying the potential mechanism of active compounds in TCM from the molecular level, and playing an important role in clinical research of TCM.

Therefore, we used network pharmacology combined with molecular docking to explore the potential mechanisms in ALRP-LSDS in the treatment of HF. The workflow was shown in Figure 1.

2. Materials and Methods

2.1. Screening of active compounds in ALRP-LSDS

"*Aconiti Lateralis Radix Praeparata*" and "*Lepidii Semen Descurainiae Semen*" were searched from the Chinese Medicine Systems Pharmacology (TCMSP) (https://tcmsp-e.com/tcmsp.php) database, which is a unique systems pharmacology platform of Chinese herbal medicines that captures the relationships between drugs, targets, and diseases,[14] as well as oral bioavailability (OB), drug-likeness (DL), and other parameters that reflect the characteristics of ADME (absorption, distribution, metabolism, and excretion).[15] OB represents the percentage of

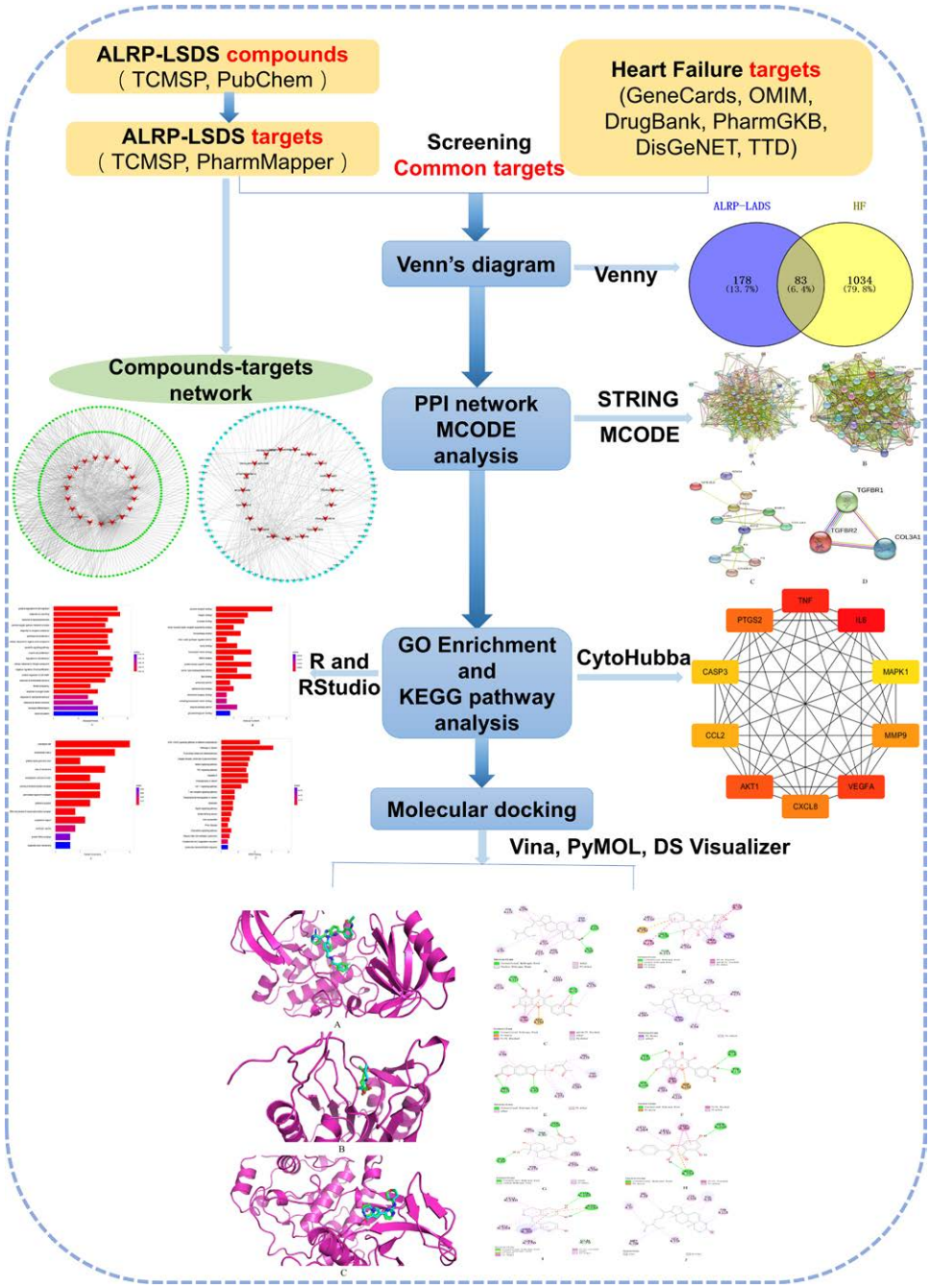

Figure 1. Workflow for ALRP-LSDS against HF. ALRP-LSDS = *Aconiti Lateralis Radix Praeparata* and *Lepidii Semen Descurainiae Semen*, HF = heart failure.

an orally administered dose of unchanged drug that reaches the systemic circulation, high OB value is often a key indicator to determine the drug-like properties of a bioactive molecule as a therapeutic agent.[16,17] DL is a qualitative concept used in drug design to estimate how "drug-like" a prospective compound is, the level of 0.18 can be used as the cutoff for the constituents of TCM.[18] According to the recommendations of TCMSP and previous studies, OB ≥ 30% and DL ≥ 0.18 were taken as the criteria for screening active compounds in TCM.

2.2. Acquisition of active compounds targets in ALRP-LSDS

The 3D structures of screened active compounds were searched and downloaded from the PubChem database (http://pubchem.ncbi.nlm.nih.gov/),[19] which is an open chemistry database online and collects information on chemical structures, identifiers, chemical and physical properties, etc. The download structures were imported into the online analysis tool PharmMapper (http://www.lilab-ecust.cn/pharmmapper/)[20] to obtain the predicted targets with a high normalized fit score (>0.9).[21] After merging the targets from TCMSP database and PharmMapper and removing the duplicate data, we finally obtained the compound targets for ALRP-LSDS. UniProt database (https://www.uniprot.org/),[22] was used to normalize the target's name and collect the UniProt ID for further analysis. The species of target proteins were set to "Homo sapiens."

2.3. Acquisition of HF targets

The keyword "heart failure" was searched in the 6 databases including the GeneCards database (https://www.genecards.org/,

ver. 5.0),[23] Online Mendelian Inheritance in Man (OMIM) (https://www.omim.org/, updated December, 2020),[24] DrugBank database (https://go.drugbank.com/),[25] PharmGKB database (https://www.pharmgkb.org/),[26] DisGeNET database (https://www.disgenet.org/, DisGeNET v6 and v7),[27] and Therapeutic Target Database (TTD) (http://db.idrblab.net/ttd/)[28] to obtain the disease targets.

Then, the overlapping targets after merging the compound-related targets and disease-related targets were regarded as the potential targets of ALRP-LSDS for the treatment of HF. UniProt database was used to normalize the target's name and collect the UniProt ID for further analysis. Venn's diagram was conducted by the online tool Venny 2.1.0. (https://bioinfogp.cnb.csic.es/tools/venny/index.html)[29] to visualize.

2.4. Construction of protein–protein interaction and MCODE module networks

The potential targets were imported into the online analysis tool STRING (https://string-db.org, ver. 11.0),[30] to find interactions between obtained potential targets. The organism was limited to "Homo sapiens" and an interaction score with medium confidence (0.400) was set to analyze the protein–protein interaction (PPI). Different colored edges represent different types of evidence.

Proteins with similar functions are usually clustered together to represent molecular biological units of function. Therefore, the function of proteins can be predicted by using the algorithm to analyze the network containing proteins with known and unknown functions.[31] Thus, we used MCODE, a plug-in of Cytoscape 3.7.0 to discover the density region of interaction in the PPI network without being affected by high false positives due to high flux technology.

2.5. Gene Ontology enrichment analysis and KEGG pathway analysis

Online analysis tool Metascape (http://metascape.org/gp/index.html, updated September 16, 2020),[32] was used to perform Gene Ontology (GO) enrichment analysis and Kyoto Encyclopedia of Genes and Genomes (KEGG) pathway analysis for the targets contained in the functional modules. Biological processes (BP), cellular components (CC), and molecular function (MF) were different parts included in the GO enrichment analysis. Metascape first identified all statistically ($P < .01$) enriched terms (can be GO or KEGG terms), accumulative hypergeometric P values, and enrichment factors were calculated and used for filtering. The remaining significant terms were then hierarchically clustered into a tree based on Kappa-statistical similarities among their gene memberships (similar to what is used in the NCI DAVID site). Then a 0.3 kappa score was applied as the threshold to cast the tree into term clusters. The terms within each cluster were exported as enriched results named "Enrichment Analysis." The results were visualized by R software (version 4.0.3) and RStudio software last.

2.6. Construction of networks

The networks were constructed and analyzed by Cytoscape 3.7.0 software, including active compounds-targets network (or compounds-targets network, C-T network); active compounds-potential targets network (or compounds-potential targets network); pathways-targets network (or P-T network); active compounds-targets pathways (or compounds-targets-pathways network, C-T-P network); hub targets network.

Table 1

Active compounds of ALRP-LSDS.

Mol ID	Molecule name	Herb	OB (%)	DL
MOL002392	Deltoin	ALRP	46.69	0.37
MOL002395	Deoxyandrographolide	ALRP	56.30	0.31
MOL002397	Karakoline	ALRP	51.73	0.73
MOL002398	Karanjin	ALRP	69.56	0.34
MOL002401	Neokadsuranic acid B	ALRP	43.10	0.85
MOL002410	Benzoylnapelline	ALRP	34.06	0.53
MOL002416	Deoxyaconitine	ALRP	30.96	0.24
MOL002419	(*R*)-Norcoclaurine	ALRP	82.54	0.21
MOL002421	Ignavine	ALRP	84.08	0.25
MOL002423	Jesaconitine	ALRP	33.41	0.19
MOL000359	Sitosterol	ALRP	36.91	0.75
MOL000538	Hypaconitine	ALRP	31.39	0.26
MOL000354	Isorhamnetin	LSDS	49.60	0.31
MOL000358	β-Sitosterol	LSDS	36.91	0.75
MOL003907	Erysimoside	LSDS	65.45	0.23
MOL003908	Cynotoxin	LSDS	99.94	0.78
MOL003927	Dihomolinolenic acid	LSDS	44.11	0.20
MOL000422	Kaempferol	LSDS	41.88	0.24
MOL000098	Quercetin	LSDS	46.43	0.28

ALRP-LSDS = Aconiti Lateralis Radix Praeparata and Lepidii Semen Descurainiae Semen, DL = drug-likeness, OB = oral bioavailability.

Table 2

Potential targets of ALRP-LSDS for treating HF.

No.	Target	No.	Target	No.	Target	No.	Target	No.	Target	No.	Target
1	ABCG2	16	CES1	31	FOS	46	MAPK1	61	PPARG	76	TGFBR2
2	ADRB2	17	CFD	32	GBA	47	MMP1	62	PTEN	77	THBD
3	AKT1	18	CHRM2	33	GJA1	48	MMP2	63	PTGS2	78	TNF
4	ALB	19	CHRM4	34	HIF1A	49	MMP3	64	PYGM	79	TP53
5	ALOX5	20	COL1A1	35	HMOX1	50	MMP9	65	RAF1	80	TTR
6	APOA2	21	COL3A1	36	ICAM1	51	MPO	66	RASA1	81	VCAM1
7	AR	22	CRP	37	IFNG	52	NFE2L2	67	SCN5A	82	VEGFA
8	BCHE	23	CXCL8	38	IGF2	53	NOS2	68	SELE	83	XDH
9	BMP2	24	CYP19A1	39	IL10	54	NOS3	69	SERPINE1		
10	CALM1	25	CYP3A4	40	IL1B	55	NR3C2	70	SOD1		
11	CASP3	26	EGFR	41	IL2	56	OLR1	71	SPP1		
12	CASP8	27	ESR1	42	IL6	57	PDE3A	72	SRC		
13	CAV1	28	F2	43	INSR	58	PLAT	73	STAT1		
14	CCL2	29	F3	44	KCNH2	59	PON1	74	TGFB1		
15	CD40LG	30	F7	45	LCN2	60	PPARA	75	TGFBR1		

ALRP-LSDS = Aconiti Lateralis Radix Praeparata and Lepidii Semen Descurainiae Semen, HF = heart failure.

2.7. Screening of hub targets

The Cytohubba plug-in of Cytoscape 3.7.0 was used to further screen the 51 targets contained in 20 enriched pathways. The plug-in uses the MCC method, which is more likely to capture more essential proteins at the top of the list[33] to score 51 targets and displays the top 10 scoring targets as the hub targets of the network.

2.8. Molecular docking

Molecular docking is to simulate the binding process of 2 or more molecules based on the "lock and key principle," which has been widely used in the docking of small molecules and proteins.

Combined with the results of PPI analysis, MCODE module analysis, pathway enrichment analysis, and hub target screening, merged with the 3 key targets with a higher degree in the C-T-P network. The overlapping targets were screened as receptors to dock with 19 active compounds in ALRP-LSDS. Download PDB files for the crystal structure of receptors and MOL2 files for the structure of active compounds (ligands) from the Research Collaboratory for Structural Bioinformatics Protein Data Bank (https://www.rcsb.org)[34] database and the TCMSP database separately. Autodock Vina was used to conduct molecular docking between active compounds and receptors,[35] and the ability of binding between active compounds and key targets were initially evaluated. PyMOL (V2.x) and DS Visualizer 2021 were used for visualization.[36]

The steps are as follows

2.8.1. Preprocessing of receptor and ligand. Auto dock tools (ADT, v1.5.6) were used to preprocess the receptor and ligand, and the center and size of the Gridbox were determined as well. Processing of ligand included adjusting charges, detecting root, and choosing torsions. Then, it was saved as pdbqt file for docking. PyMOL (V2. X) was used to remove solvent from the receptor. Then, the protein and the original ligand structure of the receptor were extracted and saved as PDB format files respectively, which were imported into ADT for pretreatment. The preprocess included adding hydrogens, computing Gasteiger, and assigning AD4 type. Then saved processed protein as pdbqt file for docking. Treatment of the original ligand is the same as that of the docking ligand.

2.8.2. Setting of the configuration file. The ligand expansion method was used to conduct semiflexible docking, and the Grid Box was set according to the location of the original ligand. Parameters such as energy range, exhaustiveness, and the number of modes were default.[37]

2.8.3. Analysis of docking result. The result with the lowest binding energy was selected as the result to further analyze the H-bond and π-π/π-H interaction. The ligand and receptor binding can form a stable structure if they are bound to 1 or more residues by the H-bond, π-H bond, or π-π bond, and participate in a conformational change, energy complementation, and other processes.[38]

3. Results

3.1. Active compounds of ALRP-LSDS

A total of 133 compounds were retrieved from the TCMSP database, 33 of which met the screening conditions of OB ≥ 30% and DL ≥ 0.18. A total of 19 active compounds with the accurate 3D structure were screened in the PubChem database, 12 active compounds of which belonged to ALRP, and 7 belonged to LSDS. Among the 14 compounds removed, 10 were lacking precise 3D structural information and the other 4 were not found (Table 1).

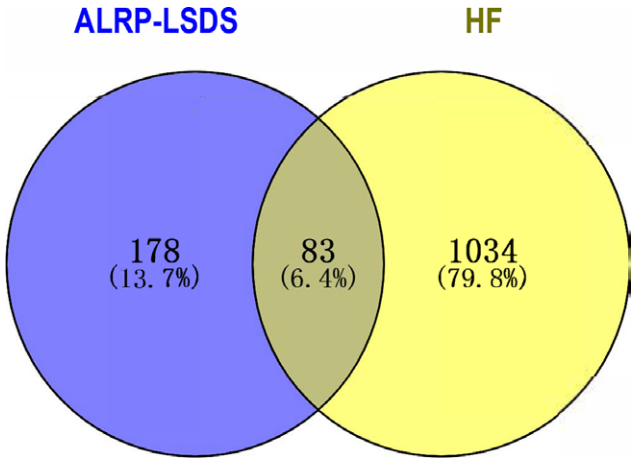

Figure 2. Venn's diagram of ALRP-LSDS for treating HF. The blue circle represents compound targets of ALRP-LSDS, which contains 261 targets. The yellow circle represents disease targets of HF, which contains 1117 targets. The overlapping part of 2 circles represents the potential targets of ALRP-LSDS for treating HF, which contains 83 targets. ALRP-LSDS = *Aconiti Lateralis Radix Praeparata* and *Lepidii Semen Descurainiae Semen*, HF = heart failure.

3.2. Screened and predicted targets of ALRP-LSDS

There were 18 screened targets and 79 predicted targets of ALRP, and 92 targets were obtained after merging and removing duplicate targets. There were 194 screened targets and 70 predicted targets of LSDS, and a total of 245 targets were obtained after merging and removing duplicates. Finally, 261 targets of active compounds of ALRP-LSDS were obtained. Of the 14 active compounds removed, relative targets of 10 compounds were not retrieved in the TCMSP database (Table S1, Supplemental Digital Content, http://links.lww.com/MD/G996).

3.3. Potential targets of ALRP-LSDS for treating HF

A total of 1260 targets related to HF were retrieved in 6 databases, 48 targets of which were obtained from the DrugBank database, 20 from the OMIM database, 13 from the PharmGKB database, 22 from the TTD database, 809 from the GeneCards database, and 248 from DiGeNET database. A total of 1117 targets were screened after merging and removing duplicate targets. Finally, 83 overlapping targets were obtained after merging 261 compound targets and 1117 HF-related targets, which were regarded as the potential targets of ALRP-LSDS for treating HF (Table 2, Fig. 2).

Table 3

Functional modules of PPI network.

Module	Average score	Nodes	Edges	Node IDs
1	24.30	39	656	IL10, HIF1A, SRC, CASP3, VEGFA, ALB, TP53, SPP1, CXCL8, PPARG, EGFR, ESR1, AKT1, IL1B, ICAM1, NOS3, IL6, TNF, FOS, MAPK1, HMOX1, MMP2, TGFB1, SERPINE1, MPO, CCL2, IL2, IFNG, CRP, VCAM1, MMP3, MMP1, NOS2, SELE, CAV1, CASP8, STAT1, PTGS2, MMP9
2	18.07	12	20	PTEN, AR, GJA1, IGF2, NFE2L2, F2, COL1A1, SOD1, F3, CD40LG, BMP2, THBD
3	10.18	3	3	COL3A1, TGFBR1, TGFBR2

PPI = protein–protein interaction.

3.4. Construction of PPI and MCODE module networks

The PPI network contained 83 nodes and 1266 edges, each node represented a target, each edge represented correlation evidence between 2 targets, and edges of different colors represented different types of correlation evidence. Disconnected nodes were not found, indicating there were direct or indirect interactions among the 83 potential targets.

Three modules were obtained from the PPI network through MCODE analysis. Module 1 contained 39 nodes and 656 edges, module 2 contained 12 nodes and 20 edges, and module 3 contained 3 nodes and 3 edges. Modules with higher average scores might play more important roles in the PPI network. So module 1 was more important with the highest score of 24.30 (Table 3, Fig. 3).

3.5. GO enrichment analysis and KEGG pathway analysis

Metascape was used to perform GO enrichment analysis and KEGG pathway analysis on 54 targets contained in the 3 modules obtained from the PPI network. They were highly enriched in 4692 BP, 426 MF, 305 CC, and 359 KEGG pathways with $P < .01$, which could deepen our understanding of targets' function at different levels. The more important BP was positive regulation of cell migration ($P = 5.89E^{-30}$), response to wounding ($4.78E^{-29}$), response to lipopolysaccharide ($1.35E^{-28}$), and reactive oxygen species metabolic process ($3.31E^{-28}$). The more important MF was cytokine receptor binding ($5.75E^{-20}$). Membrane raft ($5.13E^{-17}$) was the most important CC (Tables 4, 5, and 6, Fig. 4).

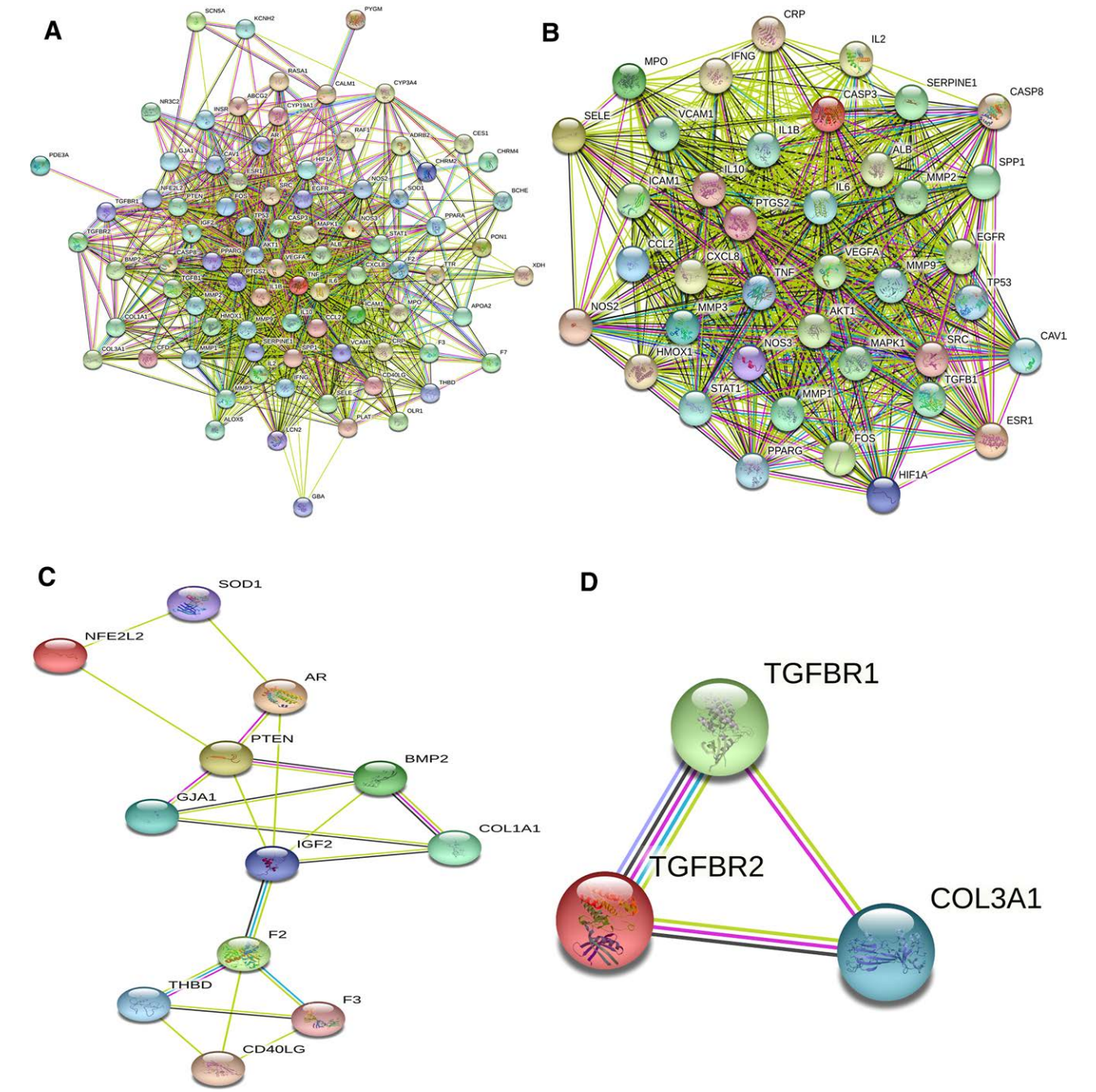

Figure 3. PPI and MCODE module networks of potential targets. (A) PPI network of 83 potential targets, contains 83 nodes and 1266 edges. (B) Module 1 of the PPI network, includes 39 nodes and 656 edges. (C) Module 2 of the PPI network, includes 12 nodes and 20 edges. (D) Module 3 of the PPI network, includes 3 nodes and 3 edges. PPI = protein–protein interaction.

Table 4

GO biological processes.

GO	Description	Count	%	*P* value
GO:0030335	Positive regulation of cell migration	26	48.15	5.89E–30
GO:0009611	Response to wounding	27	50	4.7863E–29
GO:0032496	Response to lipopolysaccharide	22	40.74	1.34896E–28
GO:0072593	Reactive oxygen species metabolic process	21	38.89	3.31131E–28
GO:0010035	Response to inorganic substance	24	44.44	1.1749E–26
GO:0050673	Epithelial cell proliferation	22	40.74	2.04174E–25
GO:0071407	Cellular response to organic cyclic compound	22	40.74	1.86209E–24
GO:0097190	Apoptotic signaling pathway	23	42.59	2.51189E–24
GO:0033002	Muscle cell proliferation	18	33.33	3.31131E–24
GO:0030155	Regulation of cell adhesion	24	44.44	5.88844E–24
GO:1901699	Cellular response to nitrogen compound	23	42.59	1.69824E–23
GO:0008285	Negative regulation of cell proliferation	24	44.44	2.75423E–23
GO:0010942	Positive regulation of cell death	23	42.59	2.39883E–22
GO:0009991	Response to extracellular stimulus	21	38.89	2.63027E–22
GO:0007565	Female pregnancy	15	27.78	1.90546E–20
GO:0070482	Response to oxygen levels	18	33.33	2.13796E–20
GO:0009612	Response to mechanical stimulus	14	25.93	2.69153E–18
GO:0048545	Response to steroid hormone	16	29.63	3.16228E–18
GO:0002521	Leukocyte differentiation	18	33.33	5.12861E–18
GO:0008015	Blood circulation	18	33.33	6.76083E–18

GO = gene ontology.

Table 5

GO Molecular function.

GO	Description	Count	%	*P* value
GO:0005126	Cytokine receptor binding	16	29.63	5.7544E–20
GO:0005178	Integrin binding	9	16.67	8.51138E–12
GO:0002020	Protease binding	8	14.81	2.29087E–10
GO:0032813	Tumor necrosis factor receptor superfamily binding	5	9.26	3.54813E–08
GO:0019902	Phosphatase binding	7	12.96	9.33254E–08
GO:0030235	Nitric-oxide synthase regulator activity	3	5.56	2.34423E–07
GO:0020037	Heme binding	6	11.11	2.75423E–07
GO:0008134	Transcription factor binding	10	18.52	3.63078E–07
GO:0046332	SMAD binding	5	9.26	4.46684E–07
GO:0019904	Protein domain-specific binding	10	18.52	9.54993E–07
GO:0004252	Serine-type endopeptidase activity	6	11.11	9.54993E–07
GO:0008289	Lipid binding	10	18.52	2.29087E–06
GO:0016209	Antioxidant activity	4	7.41	2.34423E–05
GO:0031406	Carboxylic acid binding	5	9.26	7.24436E–05
GO:0042379	Chemokine receptor binding	3	5.56	0.000338844
GO:0033613	Activating transcription factor binding	3	5.56	0.000501187
GO:0008047	Enzyme activator activity	6	11.11	0.000537032
GO:0005539	Glycosaminoglycan binding	4	7.41	0.001096478

GO = gene ontology.

Table 6

GO cellular components.

GO	Description	Count	%	*P* value
GO:0045121	Membrane raft	15	27.78	5.13E–17
GO:0031012	Extracellular matrix	12	22.22	6.92E–10
GO:0031093	Platelet alpha granule lumen	5	9.26	1.95E–07
GO:0098552	Side of membrane	10	18.52	2.82E–07
GO:0005788	Endoplasmic reticulum lumen	7	12.96	2.09E–06
GO:0098797	Plasma membrane protein complex	9	16.67	6.61E–06
GO:0048471	Perinuclear region of cytoplasm	9	16.67	9.77E–06
GO:0005912	Adherens junction	7	12.96	9.12E–05
GO:0090575	RNA polymerase II transcription factor complex	4	7.41	0.000245
GO:0099568	Cytoplasmic region	6	11.11	0.000417
GO:0030139	Endocytic vesicle	4	7.41	0.00309
GO:0032993	Protein–DNA complex	3	5.56	0.007244
GO:0031968	Organelle outer membrane	3	5.56	0.00871

GO = gene ontology.

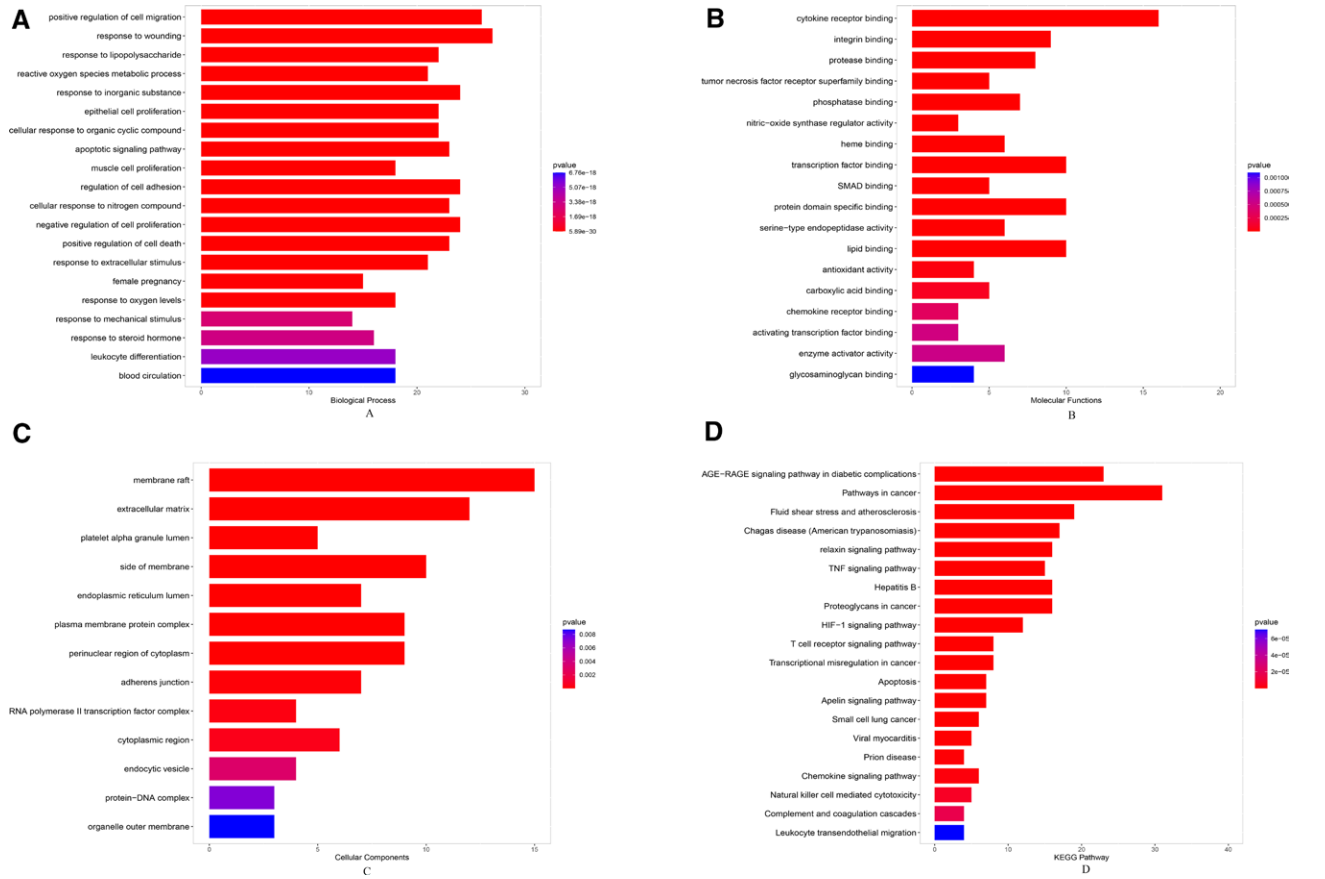

Figure 4. GO and KEGG analysis of targets in 3 clustered modules. (A) Biological process. (B) Molecular function. (C) Cellular component. (D) KEGG pathway. *Y*-axis shows significantly enriched categories of the targets and the *x*-axis shows the count of enriched targets of enriched categories ($P<.01$). The color of the columns represents the *P* value of enriched categories, the redder the column color, the smaller the *P* value. GO = gene ontology, KEGG = Kyoto Encyclopedia of Genes and Genomes.

The results of the KEGG pathway analysis showed that the AGE-RAGE signaling pathway in diabetic complications ($2.63E^{-43}$), the pathways in cancer ($1.55E^{-38}$), and the fluid shear stress and atherosclerosis ($1.12E^{-30}$) pathway were more important of ALRP-LSDS for treating HF (Table 7). In addition, 51 potential targets were enriched on the 20 enriched pathways (Figs. 5 and 7). Pathways and targets relationships were shown in the pathways-targets network, indicating pathways could work with each other through their common targets.

3.6. Network analysis

A total of 19 compounds and 261 targets were used to construct the active compounds-potential targets network of ALRP-LSDS. The network contained 280 nodes and 720 edges, showing the relationship network of active compounds and their interactive targets. The compounds with higher degrees included quercetin (degree = 163), kaempferol (degree = 72), and β-sitosterol (degree = 55), indicating they might be the main active compounds of ALRP-LSDS for the treatment of various diseases (Fig. 6).

A total of 19 compounds and 83 potential targets were used to construct the active compounds-potential targets network. The network contained 102 nodes and 227 edges, which showed the relationship between active compounds and potential targets of ALRP-LSDS for treatment of HF more clearly, compared with the active compounds-targets network. Quercetin (degree = 63), kaempferol (degree = 26), β-sitosterol (degree = 15), and deltoin (degree = 15) were connected with more targets according to the degree, indicating these compounds might be more important in the network (Fig. 7).

A total of 19 compounds, 51 enriched targets, and 20 KEGG pathways were used to construct the active compounds-targets-pathways network. The network contained 92 nodes and 380 edges. Pathways in cancer (degree = 31), AGE-RAGE signaling pathway in diabetic complications (degree = 23), Fluid shear stress and atherosclerosis (degree = 19) pathways might be the main pathways of ALRP-LSDS for the treatment of HF, which was consistent with the results of pathway enrichment analysis (Fig. 8).

3.7. Screening of hub targets

Ten hub targets were screened from 51 targets enriched by 20 KEGG pathways using the CytoHubba plug-in. The 10 hub targets were IL6, TNF, VEGFA, AKT1, PTGS2, CXCL8, MMP9, CCL2, CASP3, and MAPK1 in descending order of scores (Table 8 and Fig. 9). In addition, the 10 hub targets were all included in the targets enriched on 3 main pathways, indicating the 3 main pathways might play an important role in ALRP-LSDS for treating HF, which was consistent with the results of pathway analysis and network analysis.

3.8. Molecular docking

Panalysis results showed that the targets MAPK1 (degree = 24), CASP3 (degree = 18), and AKT1 (degree = 16) with a high degree of freedom were more important in the active compounds-targets-pathways network, which were also included in the module

Table 7

KEGG pathway analysis.

Pathway ID	Pathway name	*P* value	Count	Gene name
KEGG:04933	AGE-RAGE signaling pathway in diabetic complications	2.63E–43	23	AKT1, CASP3, COL1A1, COL3A1, F3, ICAM1, IL1B, IL6, CXCL8, MMP2, NOS3, SERPINE1, MAPK1, CCL2, SELE, STAT1, TGFB1, TGFBR1, TGFBR2, THBD, TNF, VCAM1, VEGFA
KEGG:05200	Pathways in cancer	1.55E–38	31	AKT1, AR, BMP2, CASP3, CASP8, EGFR, ESR1, F2, FOS, HIF1A, HMOX1, IFNG, GF2, IL2, IL6, CXCL8, MMP1, MMP2, MMP9, FE2L2, NOS2, PPARG, MAPK1, TEN, PTGS2, STAT1, TGFB1, TGFBR1, TGFBR2, TP53, VEGFA
KEGG:05418	Fluid shear stress and atherosclerosis	1.12E–30	19	AKT1, CAV1, FOS, HMOX1, ICAM1, IFNG, IL1B, MMP2, MMP9, NFE2L2, NOS3, CCL2, SELE, SRC, THBD, TNF, TP53, VCAM1, VEGFA
KEGG:05142	Chagas disease (American trypanosomiasis)	3.63E–29	17	AKT1, CASP8, FOS, IFNG, IL1B, IL2, IL6, CXCL8, IL10, NOS2, SERPINE1, MAPK1, CCL2, TGFB1, TGFBR1, TGFBR2, TNF
KEGG:04926	Relaxin signaling pathway	6.92E–25	16	AKT1, COL1A1, COL3A1, EGFR, FOS, MMP1, MMP2, MMP9, NOS2, NOS3, MAPK1, SRC, TGFB1, TGFBR1, TGFBR2, VEGFA
KEGG:04668	TNF signaling pathway	1.74E–24	15	AKT1, CASP3, CASP8, FOS, ICAM1, IL1B, IL6, MMP3, MMP9, MAPK1, PTGS2, CCL2, SELE, TNF, VCAM1
KEGG:05161	Hepatitis B	5.62E–23	16	AKT1, CASP3, CASP8, FOS, IL6, CXCL8, MMP9, MAPK1, PTEN, SRC, STAT1, TGFB1, TGFBR1, TGFBR2, TNF, TP53
KEGG:05205	Proteoglycans in cancer	1.70E–21	16	AKT1, CASP3, CAV1, EGFR, ESR1, HIF1A, IGF2, IL6, MMP2, MMP9, MAPK1, SRC, TGFB1, TNF, TP53, VEGFA
KEGG:04066	HIF-1 signaling pathway	5.75E–18	12	AKT1, EGFR, F3, HIF1A, HMOX1, IFNG, IL6, NOS2, NOS3, SERPINE1, MAPK1, VEGFA
KEGG:04660	T-cell receptor signaling pathway	2.29E–11	8	AKT1, CD40LG, FOS, IFNG, IL2, IL10, MAPK1, TNF
KEGG:05202	Transcriptional misregulation in cancer	2.04E–09	8	IL6, CXCL8, MMP3, MMP9, MPO, PPARG, TGFBR2, TP53
KEGG:04210	Apoptosis	8.91E–09	7	AKT1, CASP3, CASP8, FOS, MAPK1, TNF, TP53
KEGG:04371	Apelin signaling pathway	1.32E–08	7	AKT1, NOS2, NOS3, SERPINE1, MAPK1, SPP1, TGFBR1
KEGG:05222	Small cell lung cancer	3.80E–08	6	AKT1, CASP3, NOS2, PTEN, PTGS2, TP53
KEGG:05416	Viral myocarditis	2.45E–07	5	CASP3, CASP8, CAV1, CD40LG, ICAM1
KEGG:05020	Prion diseases	6.17E–07	4	IL1B, IL6, MAPK1, SOD1
KEGG:04062	Chemokine signaling pathway	1.38E–06	6	AKT1, CXCL8, MAPK1, CCL2, SRC, STAT1
KEGG:04650	Natural killer cell mediated cytotoxicity	5.89E–06	5	CASP3, ICAM1, IFNG, MAPK1, TNF
KEGG:04610	Complement and coagulation cascades	1.66E–05	4	F2, F3, SERPINE1, THBD4
KEGG:04670	Leukocyte transendothelial migration	7.08E–05	4	ICAM1, MMP2, MMP9, VCAM1

KEGG = Kyoto Encyclopedia of Genes and Genomes.

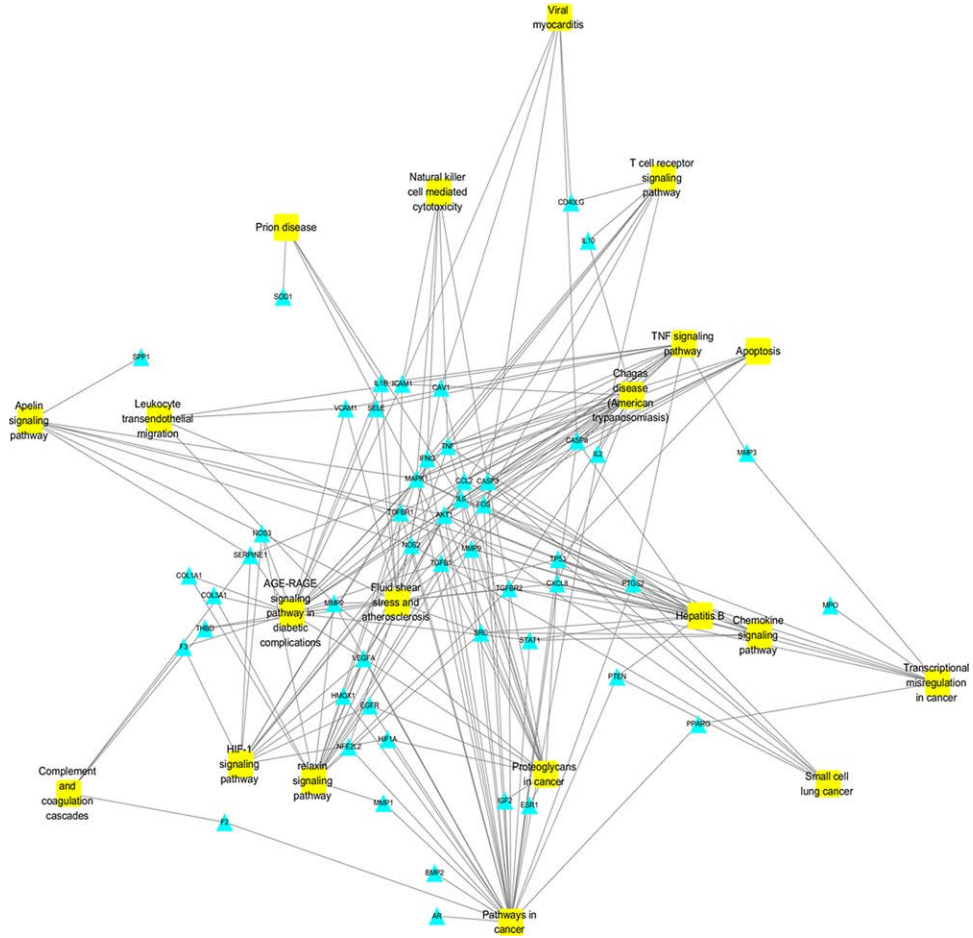

Figure 5. Pathways-targets network of KEGG pathway analysis. The yellow rectangles represent the 20 pathways obtained in enrichment results, the blue triangles represent targets on 20 enriched pathways, and the edges represent interactions among targets and pathways. KEGG = Kyoto Encyclopedia of Genes and Genomes.

1 and the AGE-RAGE signaling pathway in diabetic complications. In addition, human crystal structures containing co-crystal ligands of 3 targets were also found in the PDB database. Therefore, AKT1 (PDB ID: 4EJN), CASP3 (PDB ID: 2XYH), and MAPK1 (PDB ID: 5NHV) were finally selected as docking receptors with 19 active compounds of ALRP-LSDS, respectively. The docking ligand and original ligand were almost identical among the 3 receptors, indicating the rationality of docking parameters and the reliability of docking results (Fig. 10). Docking results were shown in Table 9. The negative binding energy indicated the active compounds of ALRP-LSDS could bind to AKT1, CASP3, and MAPK1 spontaneously. Ten active compounds showed a good binding ability to key targets, such as β-sitosterol (−10.8 kcal·mol), karanjin (−10.2 kcal·mol), isorhamnetin (−9.7 kcal·mol), etc, of which 5 belonged to ALRP and 5 belonged to LSDS. In addition, AKT1 showed a better binding ability to active compounds compared with the other 2 key targets. β-Sitosterol combined better with MAPK1 and AKT1, while karanjin combined better with CASP3. According to the formation of chemical bonds (mainly H-bonds, π-π or π-H bond), the binding between β-sitosterol, karanjin, isorhamnetin, deltoin, quercetin, deoxyandrographolide, kaempferol, (*R*)-norcoclaurine and key targets is more stable. Two H-bonds were formed between β-sitosterol and Asn204, Ser205 residues of AKT1. Karanjin forms an H-bond with Ser205 residue of AKT1 and 2 π-π bonds with Trp80 and Tyr272 residues. Isorhamnetin forms 2 H-bonds with Thr211 and Gln79 residues, and 1 π-π stacking with Trp80 residue. Two H-bonds were formed between Deltoin and Arg273, Thr82 residues of AKT1. Four H-bonds were formed between Quercetin and Ser272, Asn54, Ser205, Thr211 residues, and 1 π-π stacking was formed between Quercetin and Trp80 residue. There were 2 H-bonds between deoxyandrographolide and Ser205, Thr82 residues of AKT1. Kaempferol formed 2 H-bonds with Ser205 and Asp292 residues of AKT1 and formed 1 π-π stacking with Trp80 residue. Two H-bonds were formed between (*R*)-norcoclaurine and Thr291, Asp292 residues of AKT1 (Fig. 11).

In addition, by comparing the docking ability of core targets MAPK1, CASP3, and AKT1 with their original ligands and active compounds, we found that the binding ability of β-sitosterol to MAPK1, and karanjin to CASP3 were better than its original ligand (Table 10).

4. Discussion

The results showed that β-sitosterol, karanjin, isorhamnetin, quercetin, deltoine, kaempferol, dehydroandrographolide, and (*R*)-noraconitine all formed H-bonds with the key targets. In addition, karanjin, isorhamnetin, quercetin, kaempferol, and (*R*)-noraconitine also formed a π-π bond with the key targets. The bond between the 8 active compounds with key targets is more stable, indicating the 8 compounds might be the main active compounds of ALRP-LSDS for treating HF.

The efficacy of ALRP-LSDS for treating HF has been verified by experiments.[39,40] The compound β-sitosterol is one of the alcohols of LSDS, while isorhamnetin, quercetin, and kaempferol are all flavonoids, which are the main components of LSDS. Quercetin has the highest content in flavonoids.[41–43] Studies have shown that quercetin can inhibit myocardial hypertrophy and the mechanism

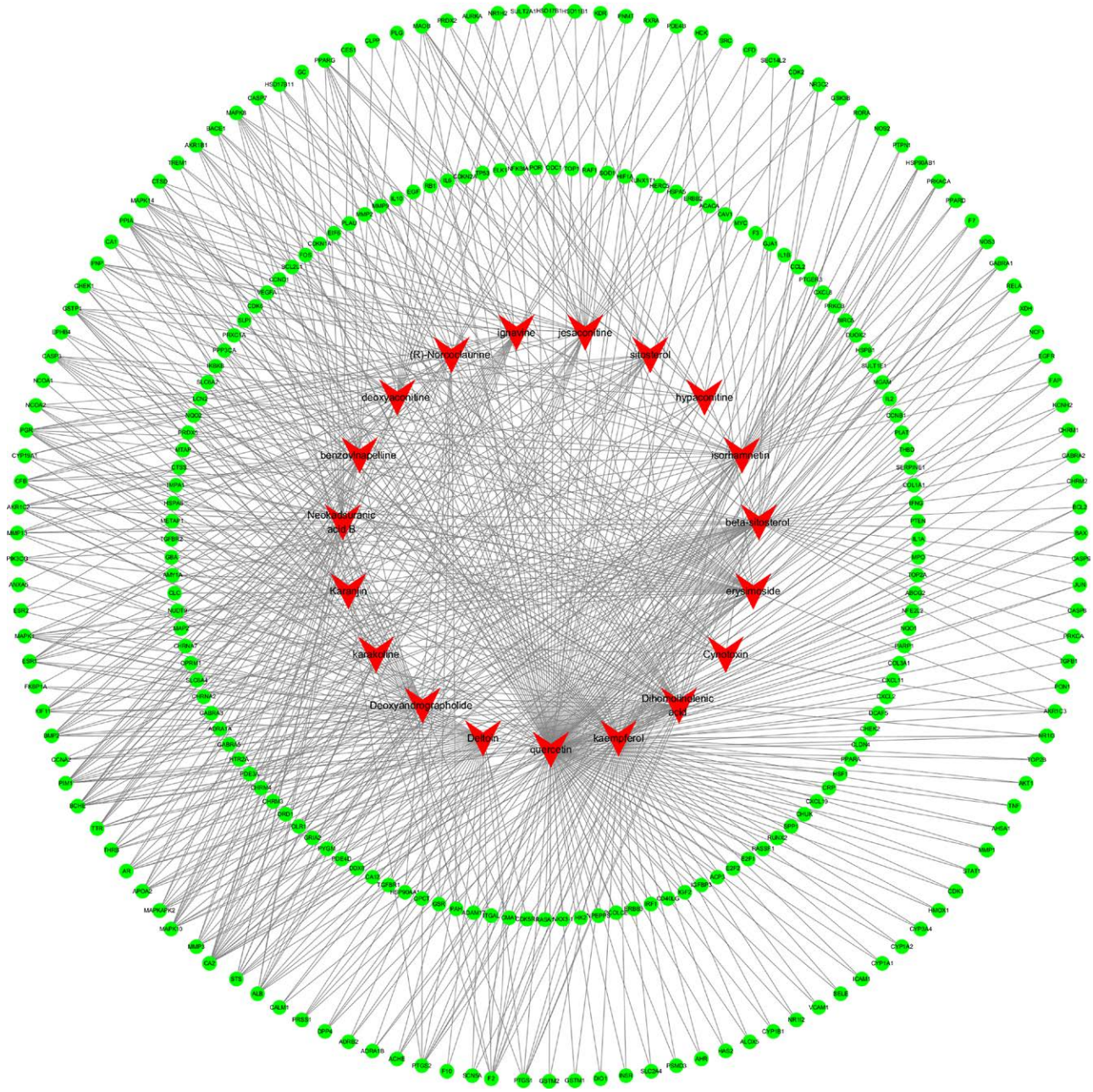

Figure 6. Active compounds-targets network of ALRP-LSDS. Red arrows represent active compounds of ALRP-LSDS. Green circles represent targets of ALRP-LSDS. Edges represent the interaction between active compounds and targets. ALRP-LSDS = *Aconiti Lateralis Radix Praeparata* and *Lepidii Semen Descurainiae Semen*.

may be related to the activation of GSK-3β and proteasome activity by inhibiting the activity of Akt.[44,45] Kaempferol can inhibit cardiomyocytes apoptosis and the oxidative stress of hypoxic cardiomyocytes.[46,47] Isorhamnetin has cardiovascular protective effects such as dilating coronary artery,[48] suppressing the thrombosis and platelet aggregation.[49] The alcohols of LSDS can enhance myocardial contractility, suppress heart rate, and improve cardiovascular function, which may be closely related to improving oxidative stress imbalance and preventing over activation of the neuroendocrine system.[39,50]

The other 4 active compounds, karanjin, deltoine, deoxyandrographolide, and (*R*)-noraconitine were derived from ALRP. The main components of ALRP include alkaloids, flavonoids, saponins, etc. The alkaloids of ALRP benefit cardiovascular diseases.[51] (*R*)-noraconitine belongs to the alkaloids of ALRP,[52] which can be used as a β-adrenergic receptor agonist to activate the β-adrenergic receptor and exert a cardiotonic effect.[53] Although karanjin, deltoine, and dehydroandrographolide are also important compounds with good binding ability, their influence on the treatment of HF has not been reported nowadays and further research is necessary. In addition, the cardiotonic effect of karakoline, hypaconitine, deoxyaconitine, and other alkaloids have been reported[52] although their binding ability is relatively poor (supplementary Tables S2 and S3, Supplemental Digital Content, http://links.lww.com/MD/G996).

The target MAPK1, CASP3, and AKT1 were critical targets of ALRP-LSDS in treating HF shown in this study. AKT (also known as protein kinase B, PKB) is a serine threonine kinase, which seems to be in the critical position between various stimulants and effectors related to heart function in normal and diseased hearts. It can regulate the growth, survival, metabolism, gene expression, and contractility of the

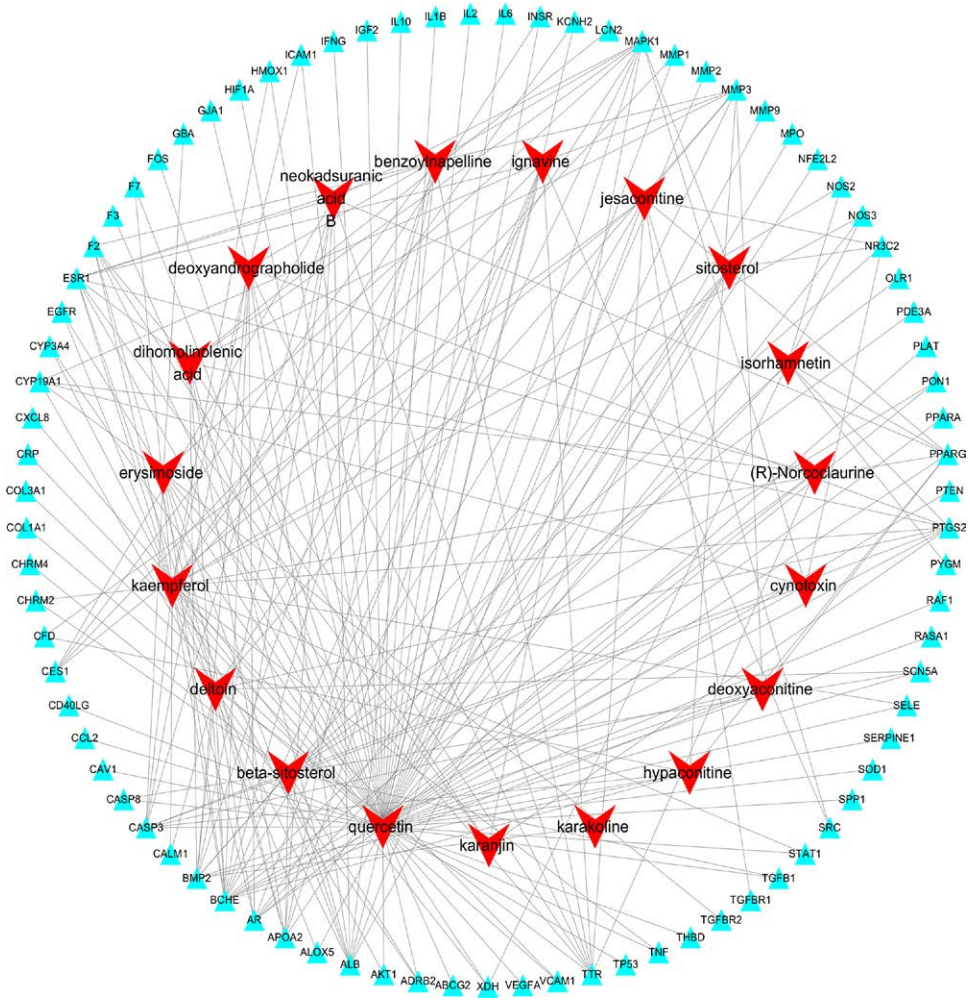

Figure 7. Active compounds-potential targets network of ALRP-LSDS for treating HF. The red arrows represent active compounds of ALRP-LSDS. Blue triangles represent potential targets of ALRP-LSDS for the treatment of HF. Edges represent the interaction between compounds and potential targets. ALRP-LSDS = *Aconiti Lateralis Radix Praeparata* and *Lepidii Semen Descurainiae Semen*, HF = heart failure.

heart.[54,55] AKT1, one of the subtypes of AKT, is the most abundant and most focused subtype of AKT and is widely expressed in the brain, heart, and lung.[56,57] The functions of AKT1 such as promoting the growth and proliferation of cardiomyocytes,[58,59] promoting physiological myocardial hypertrophy, resisting pathological myocardial hypertrophy,[60] improving systolic function, inhibiting cardiomyocyte apoptosis, and strengthening cardiac repair have been proved already.[61] Therefore, regulating the activation of AKT1 may delay REM and improve the prognosis of HF.

CASP3 is a key protease in apoptosis and plays a key role in the cascade of apoptotic proteases.[62] Activated AKT can phosphorylate proapoptotic factor bad of the B-cell lymphoma-2 (Bcl-2) family, which can bind to 14-3-3 protein in the cytoplasm to free antiapoptotic Bcl-2 or B-cell lymphoma extra large (Bcl-XL), thereby preventing the change of mitochondrial membrane permeability and the release of endogenous mitochondrial apoptotic factor, prevent apoptosis factor activated Caspase-3/6/7 (cysteiny aspartate-specific protein-6/cysteiny aspartate-specific protein-7), plays an antiapoptotic role.[63] Previous experiments showed that Fuxin decoction could upregulate the expression of Bcl-2 protein,[64] to block the process of apoptosis, protect cardiomyocytes and delay REM and play a therapeutic role.

MAPK1 (also known as mitogen-activated protein kinase 1, ERK2) is an important part of the MAP kinase signal transduction pathway. MAPK1 plays an important role in the MAPK/ERK cascade, which regulates cell growth, development, division, and other physiological and pathological processes as well as inflammatory reactions through the MAPK signaling pathway.[65,66] Our study showed that the Fuxin mixture can inhibit the expression of Raf, MEK, and ERK, thereby intervening in the process of REM through Raf/MEK/ERK pathway and delaying the development of HF.[7]

The results of pathway analysis showed that the 3 pathways with high enrichment degree were the AGE-RAGE signaling pathway in diabetic complications, Pathways in cancer, Fluid shear stress, and atherosclerosis. The 3 pathways contain 10 hub targets, all of which contain the key target AKT1.

The results of pathway analysis indicated the important pathways were the AGE-RAGE signaling pathway in diabetic complications, Pathways in cancer, and Fluid shear stress and atherosclerosis. All of the 3 pathways contained 10 hub targets, especially the key target AKT1.

AGE (advanced glycation end products) bind to RAGE (receptor for advanced glycation end products) elicits activation of multiple intracellular signal pathways involving NADPH oxidase, protein kinase C, and MAPKs, then resulting in NF-kappaB activity. NF-kappa B promotes the expression of proinflammatory cytokines such as IL1, IL6, and TNF-alpha and a variety of atherosclerosis-related genes, including VEGF, RAGE, etc. In addition, JAK-STAT-mediated and PI3K-Akt-dependent pathways are induced via RAGE, which in turn participate in cell proliferation and apoptosis respectively.[67] These 2 pathways were also enriched with $P < .01$. Besides, the experimental results

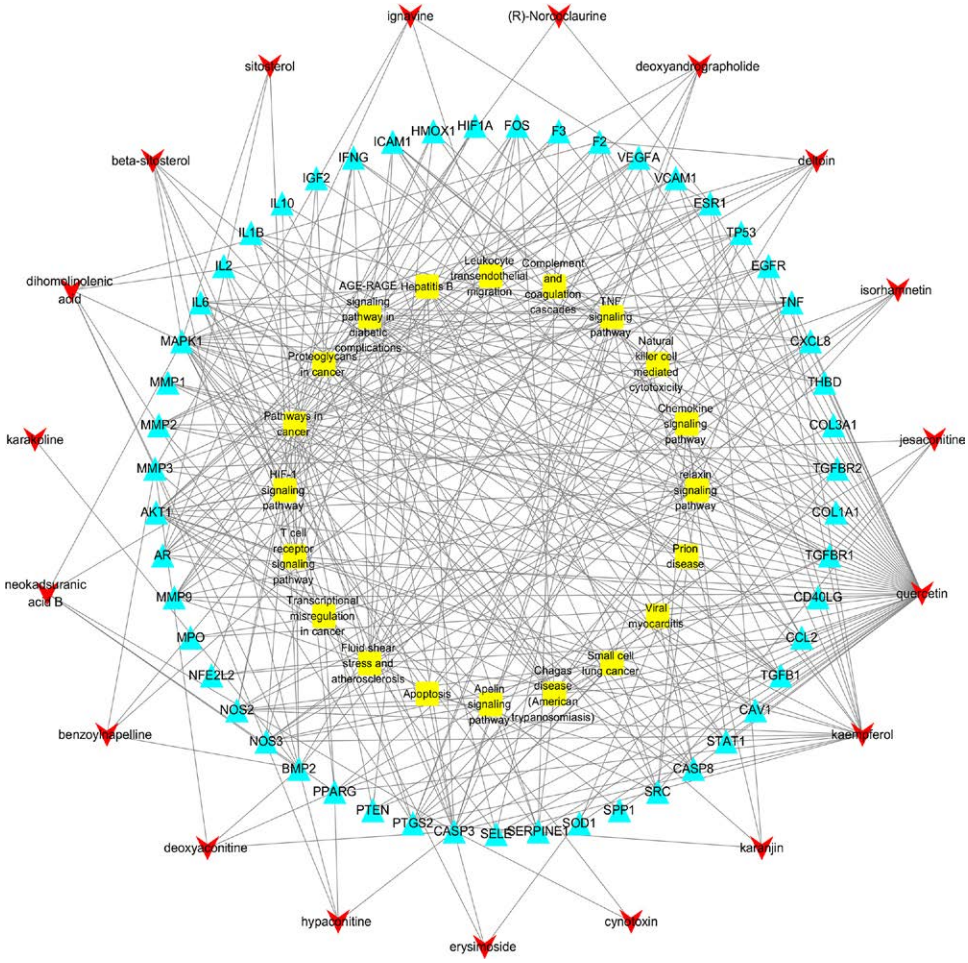

Figure 8. Active compounds-targets-pathways network of ALRP-LSDS for treating HF. The red arrows represent active compounds of ALRP-LSDS. Blue triangles represent potential targets enriched on 20 KEGG pathways. Yellow round rectangles represent 20 KEGG pathways. Edges represent interaction among active compounds, targets, and pathways. ALRP-LSDS = *Aconiti Lateralis Radix Praeparata* and *Lepidii Semen Descurainiae Semen*, HF = heart failure, KEGG = Kyoto Encyclopedia of Genes and Genomes.

Table 8

Top 10 hub targets.

Rank	Name	Score	Rank	Name	Score
1	IL6	2.56E+22	6	CXCL8	2.56E+22
2	TNF	2.56E+22	7	MMP9	2.56E+22
3	VEGFA	2.56E+22	8	CCL2	2.56E+22
4	AKT1	2.56E+22	9	CASP3	2.56E+22
5	PTGS2	2.56E+22	10	MAPK1	2.56E+22

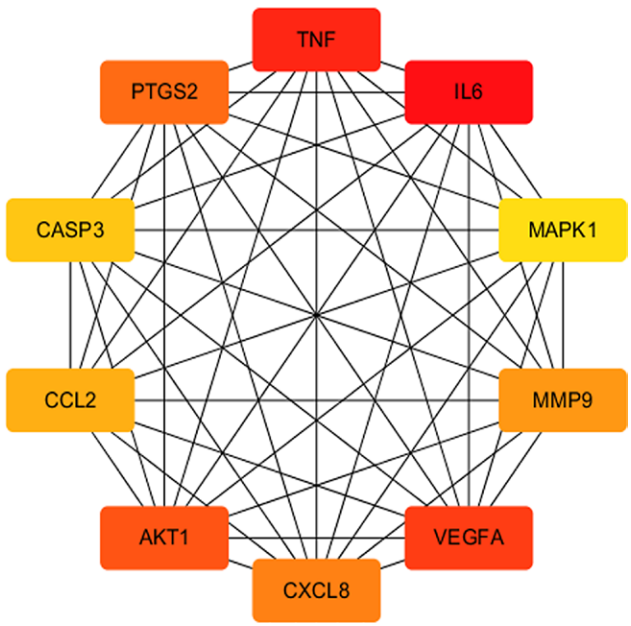

Figure 9. Network of 10 hub targets. The round rectangles represent hub targets, the redder the rectangle color, the higher the rank. Edges represent interactions among hub targets.

also indicated that Fuxin Decoction and Qiliqiangxin capsule contained ALRP-LSDS could reduce mitochondrial-dependent myocardial apoptosis induced by oxidative stress through PI3K/Akt/GSK-3β signaling pathway,[68] played a role in myocardial protection, which was beneficial to improve REM and delay the process of HF.

Besides, AGEs are also important in the occurrence and development of HF.[69] It may inhibit cardiomyocyte apoptosis and delay REM by reducing the absorption of glucose, reducing the generation of AGEs in vivo. The DAPA-HF study showed that dagliazin, a sodium glucose cotransporter 2 inhibitor (SGLT-2i), reduced hospitalization rate and overall mortality of HF/cardiovascular death in HF patients with reduced ejection fraction, in both diabetic and nondiabetic patients.[70] In addition, the use of SGLT-2 inhibitors was also recommended in HF patients with or without type 2 diabetes by the latest guidelines.[71] Therefore,

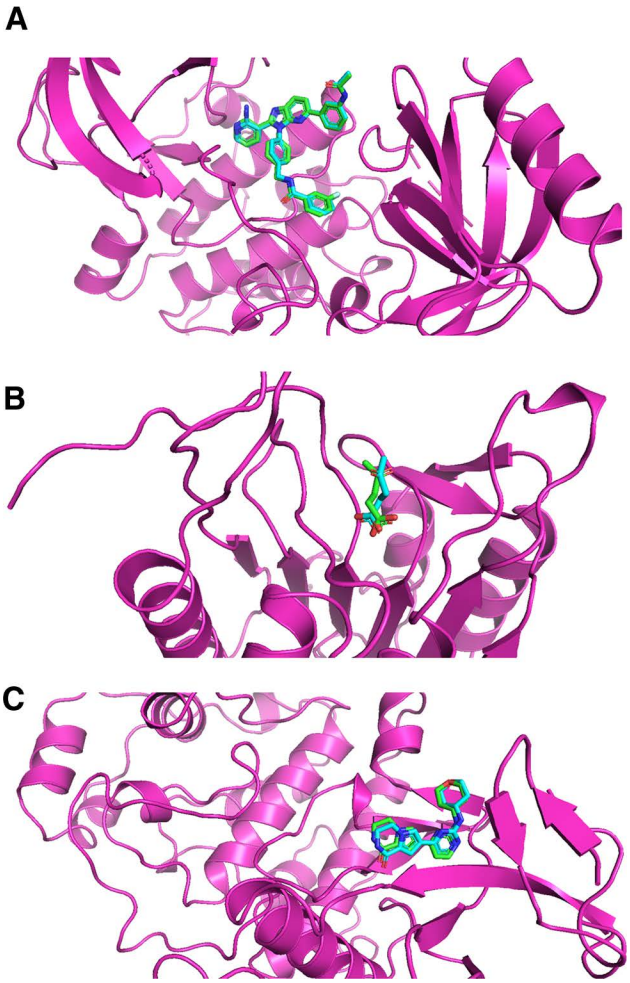

Figure 10. Comparison of the fitness of original ligand and docking ligand of key targets. (A) MAPK1 docking with 8QB. (B) CASP3 docking with TQ9. (C) AKT1 docking with 0R4. The green small molecule represents the original ligand, the blue small molecule represents the best conformation of the docking ligand. The pink molecule represents receptor protein targets.

the regulation of blood glucose and related pathways may benefit the treatment of HF.

The shear stress represents the friction exerted by the blood flow on the endothelial surface of the vascular wall, plays a central role in vascular biology, and contributes to the development of atherosclerosis. With disturbed blood flow and associated reciprocating, low shear stress often upregulate endothelial cell (EC) genes and proteins, thereby promoting the oxidation and

Table 9

Results of docking between active compounds and key targets.

Compound	Binding energy (kcal mol)	Target	Herb	Hydrogen bond	π-π/ π-H bond
β-Sitosterol	−10.8	AKT1	LSDS	Yes	–
Karanjin	−10.2	AKT1	ALRP	Yes	Yes
Isorhamnetin	−9.7	AKT1	LSDS	Yes	Yes
Sitosterol	−9.6	AKT1	ALRP	–	–
Deltoin	−9.5	AKT1	ALRP	Yes	–
Quercetin	−9.4	AKT1	LSDS	Yes	Yes
Deoxyandrographolide	−9.2	AKT1	ALRP	Yes	–
Kaempferol	−9.2	AKT1	LSDS	Yes	Yes
(*R*)-Norcoclaurine	−9.1	AKT1	ALRP	Yes	Yes
β-Sitosterol	−9.1	MAPK1	LSDS	–	–

ALRP = Aconiti Lateralis Radix Praeparata, LSDS = Lepidii Semen Descurainiae Semen.

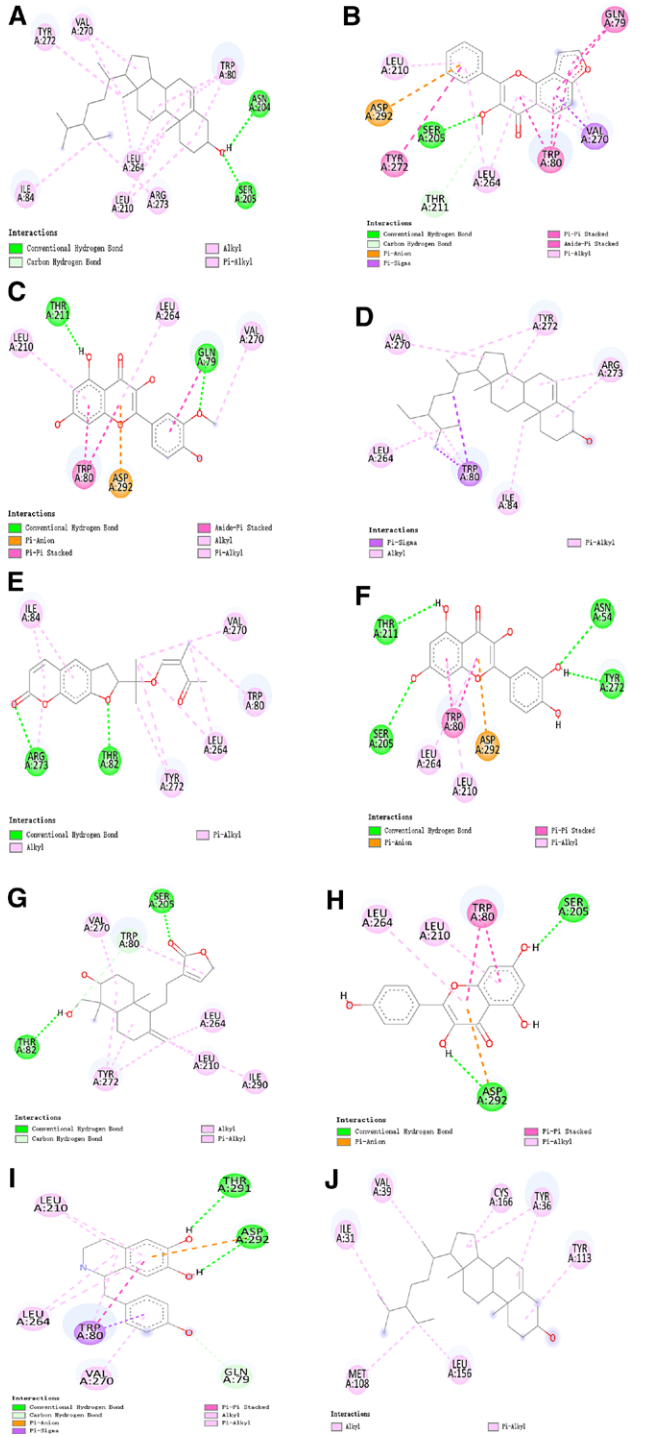

Figure 11. Docking of active compounds from ALRP-LSDS for treating HF and key targets. (A) AKT1 and β-sitosterol. (B) AKT1 and karanjin. (C) AKT1 and isorhamnetin. (D) AKT1 and sitosterol. (E) AKT1 and deltoin. (F) AKT1 and quercetin. (G) AKT1 and deoxyandrographolide. (H) AKT1 and kaempferol. (I) AKT1 and (*R*)-norcoclaurine. (J) MAPK1 and β-sitosterol. ALRP-LSDS = *Aconiti Lateralis Radix Praeparata* and *Lepidii Semen Descurainiae Semen*, HF = heart failure.

inflammation of the arterial wall, leading to atherosclerosis.[72] When ischemia and infarction occur, atherosclerotic plaques cause REM,[73] which may ultimately lead to the development of HF. Therefore, the intervention of this pathway may improve cardiovascular function and prevent HF thereby.

The Pathways in cancer appear no direct business with HF. But the targets enriched in this pathway, including AKT1,

Table 10

Docking between original ligand/compound and key targets.

Original ligand	Binding energy (kcal mol)	Target	Compound	Binding energy (kcal mol)
8QB	−8.5	MAPK1	β-Sitosterol	−9.1
TQ9	−4.7	CASP3	Karanjin	−7.4
0R4	−14.0	AKT1	β-Sitosterol	−10.8

CASP3, MAPK1, EGFR, and IL6, can participate in many BP, such as apoptosis and inflammatory response, and play a role in HF and cancer progression.[74] Therefore, the Pathways in cancer may participate in REM through the regulation of these common BP, then affect the occurrence and development of HF.

In addition, previous experiments also confirmed that Fuxin decoction could benefit HF treatment by activating the cAMP signaling pathway[9] and reducing the level of TNF-α,[75] which is consistent with the results of this study. Therefore, the network pharmacology approach is scientific and reliable.

5. Conclusion

The β-sitosterol, isorhamnetin, quercetin, kaempferol, and (*R*)-noraconitinemain may be the main active compounds of ALRP-LSDS for the treatment of HF. The key targets of it include AKT1, MAPK1, and CASP3, and the main pathways of it include the AGE-RAGE signaling pathway in diabetic complications, Pathways in cancer, and Fluid shear stress and atherosclerosis. The functions of ALRP-LADS on delaying REM and treating HF may play through multi-compounds, multi-targets, and multi-pathways, which require further research to confirm.

Author contributions

XYT and SYM conceived and designed the study. YMQ, CC, LY and ZX searched and collected the data. YMQ, CC and YYD performed the data analysis. YMQ, CC and MYF wrote and modified the manuscript. All authors are responsible for reviewing data. All authors read and approved the final manuscript.
Conceptualization: Yi-Tao Xue, Yong-Mei Song.
Data curation: Meng-Qi Yang, Xia Zhong, Yan Li.
Formal analysis: Meng-Qi Yang, Yi-Ding Yu.
Methodology: Cong Chen.
Writing – original draft: Meng-Qi Yang.
Writing – review & editing: Cong Chen, Yi-Fei Mao.

References

[1] Metra M, Teerlink JR. Heart failure. Lancet. 2017;390:1981–95.
[2] Schirone L, Forte M, Palmerio S, et al. A review of the molecular mechanisms underlying the development and progression of cardiac remodeling. Oxid Med Cell Longev. 2017;2017: 3920195
[3] Cokkinos DV, Pantos C. Myocardial remodeling, an overview. Heart Fail Rev. 2011;16:1–4.
[4] Yang JF, Wang H. The past, present and future of heart failure. Chin J Cardiol. 2017;45:688–92.
[5] Shi J, Wang X, Zhao HH, et al. Analysis of modern clinical medication law of chronic heart failure in recent 20 years. J Beijing Univ Tradit Chin Med. 2020;43:841–8.
[6] Li X, Zhang J, Huang J, et al. A multicenter randomized double-blind parallel-group placebo-controlled study of the effects of qili qiangxin capsules in patients with chronic heart failure. J Am Coll Cardiol. 2013;62:1065–72.
[7] Xue YT, Li QS, Jiao HC, et al. The effect of fuxin mixture on raf-MEK-ERK Pathway in Chronic Congestive Heart Failure (CHF) rats. Chin Archives of Tradit Chin Med. 2015;33:791–4.
[8] Xue YT,Chen W,Liu P. et al, Effects of 'Fuxin Decotion' on the expression of PI3K-AKT-GSK3β pathway in heart failure rats. Shanghai J Tradit Chin Med. 2015;49:74–78.
[9] Xue YT, Li Y, Jiao HC, et al. Effect of fuxin mixture on the β1-AR-cAMP-PKA pathway of rats with heart failure. Chin J Integr Tradit Chin Med. 2017;37:453–7.
[10] Gao T, Xue YT. Study on the mechanism of mitochondrial permeability transition hole in rats with heart failure treated by fuxin decoction. Liaoning J Tradit Chin Med. 2021;48:178–182+224.
[11] Lee CF, Tian R. Mitochondrion as a target for heart failure therapy-role of protein lysine acetylation.. Circ J. 2015;79:1863–70.
[12] Zhang Z, Yi P, Huang J, et al. Integrated network pharmacology analysis and serum metabolomics to reveal the cognitive improvement effect of bushen tiansui formula on Alzheimer's disease. J Ethnopharmacol. 2019;1:112371.
[13] Li S, Zhang B. Traditional Chinese medicine network pharmacology: theory, methodology and application. Chin J Nat Med. 2013;11:11–20.
[14] Ru JL, Li P, Wang JN, et al. TCMSP: a database of systems pharmacology for drug discovery from herbal medicines. J Cheminform. 2014;16:13.
[15] Huang C, Zheng CL, Li Y, et al. Systems pharmacology in drug discovery and therapeutic insight for herbal medicines. Brief Bioinform. 2014;15:710–33.
[16] Xu X, Zhang WX, Huang C, et al. A novel chemometric method for the prediction of human oral bioavailability. Int J Mol Sci . 2012;13:6964–82.
[17] You JS, Li CY, Chen W, et al. A network pharmacology-based study on Alzheimer disease prevention and treatment of qiong yu gao. BioData Min. 2020;13:2
[18] Tao WY, Xu X, Wang X, et al. Network pharmacology-based prediction of the active ingredients and potential targets of Chinese herbal radix curcumae formula for application to cardiovascular disease. J Ethnopharmacol. 2013;145:1–10.
[19] Kim S, Thiessen PA, Bolton EE, et al. PubChem substance and compound databases. Nucleic Acids Res. 2016;44:D1202–13.
[20] Wang X, Shen YH, Wang SW, et al. PharmMapper 2017 update: a web server for potential drug target identification with a comprehensive target pharmacophore database. Nucleic Acids Res. 2017;45:W356–60.
[21] Zhao HS, Shan YH, Ma Z, et al. A network pharmacology approach to explore active compounds and pharmacological mechanisms of epimedium for treatment of premature ovarian insufficiency. Drug Des Devel Ther. 2019;13:2997–3007.
[22] UniProt Consortium. UniProt: a worldwide hub of protein knowledge. Nucleic Acids Res. 2019;47:D506–15.
[23] Rebhan M, Chalifa-Caspi V, Prilusky J, et al. GeneCards: a novel functional genomics compendium with automated data mining and query reformulation support. Bioinformatics. 1998;14:656–64.
[24] Ada H, Scott AF, Amberger JS, et al. Online mendelian inheritance in man (OMIM), a knowledgebase of human genes and genetic disorders. Nucleic Acids Res. 2002;30:52–5.
[25] Wishart DS, Feunang YD, Guo AC, et al. DrugBank 5.0: a major update to the drugbank database for 2018. Nucleic Acids Res. 2018;46:D1074–82.
[26] Whirl-Carrillo M, McDonagh EM, Hebert JM, et al. Pharmacogenomics knowledge for personalized medicine. Clin Pharmacol Ther. 2002;92:414–7.
[27] Piñero J, Ramírez-Anguita JM, Saüch-Pitarch J, et al. The disGeNET knowledge platform for disease genomics: 2019 update. Nucleic Acids Res. 2020;48:D845–55.
[28] Wang YX, Zhang S, Li FC, et al. Therapeutic target database 2020: enriched resource for facilitating research and early development of targeted therapeutics. Nucleic Acids Res. 2020;48:D1031–41.
[29] J. C. Oliveros, Venny. An interactive tool for comparing lists with Venn's diagrams. 2007-2015. Available at: https://bioinfogp.cnb.csic.es/tools/venny/index.html [access date January 29, 2021].
[30] Szklarczyk D, Gable AL, Lyon D, et al. STRING v11: protein-protein association networks with increased coverage, supporting functional discovery in genome-wide experimental datasets. Nucleic Acids Res. 2019;47:D607–13.
[31] Altaf-Ul-Amin M, Shinbo Y, Mihara K, et al. Development and implementation of an algorithm for detection of protein complexes in large interaction networks. BMC Bioinf. 2006;7:207.
[32] Zhou YY, Zhou B, Pache L, et al. Metascape provides a biologist-oriented resource for the analysis of systems-level datasets. Nat Commun. 2019;10:1523.
[33] Chin CH, Chen SH, Wu HH, et al. CytoHubba: identifying hub objects and sub-networks from complex interactome. BMC Syst Biol. 2014;8(Suppl 4):S11.
[34] Berman HM, Westbrook J, Feng Z, et al. The protein data bank. Nucleic Acids Res. 2000;28:235–42.

[35] Trott O, Olson AJ. AutoDock vina: improving the speed and accuracy of docking with a new scoring function, efficient optimization, and multithreading. J Comput Chem. 2010;31:455–61.
[36] Seeliger D, de Groot BL. Ligand docking and binding site analysis with PyMOL and Autodock/Vina. J Comput Aided Mol Des. 2010;24:417–22.
[37] Forli S, Huey R, Pique ME, et al. Computational protein–ligand docking and virtual drug screening with the autodock suite. nat protoc,. Nat Protoc. 2016;11:905–19.
[38] Yan W, Li SX, Wei MJ, et al. Identification of MMP9 as a novel key gene in mantle cell lymphoma based on bioinformatic analysis and design of cyclic peptides as MMP9 inhibitors based on molecular docking. Oncol Rep. 2018;40:2515–24.
[39] Zhang GS, Bai YP, Wang XL, et al. Effective fractions and mechanism of descurainiae semen lepidii semen in chronic heart failure rats.. Chin J Experimental Tradit Med Formulae. 2017;23:118–25.
[40] Zhou YX, Peng C, Liu JL, et al. Hemodynamic effect of fupian fluid on model of rats with acute heart failure. J Emerg Tradit Chin Med. 2014;23:382–4.
[41] Zhou XD, Tang LY, Zhou GH, et al. Advances on lepidii semen and descurainiae semen. China J Chin Materia Medica. 2014;39:4699–708.
[42] K. Sun, Studies of the constituents and biological activities of Descurainia Sophia (L.). Shenyang, China: Shenyang Pharmaceutical University. 2005.
[43] Ma MF, Zhang DZ, Li J. Simultaneous determination of quercetin kaempferol and isorhamnetin in descurainia sophia (L.) Webb ex Prantl by HPLC. Chin Archives of Tradit Chin Med. 2010;28:2210–12.
[44] Ham JJ, Hao J, Kim CH, et al. Quercetin prevents cardiac hypertrophy induced by pressure overload in rats. J Vet Med Sci. 2009;71:737–43.
[45] Chen KX, Li SJ, Luo JD, et al. Quercetin attenuates cardiomyocyte hypertrophy through proteasome inhibition. Chin J Pathophysiol. 2015;31:1352–59.
[46] Zhao CC, Zhang J, Han WN, et al. Effect of kaempferol, apigenin on injury of mitochondria in H2O2-induced cardiomyocyte apoptosis. Chin J Pathophysiol. 2008;24:1434–33.
[47] Yu X, Guo SZ, Shi TJ, et al. Protective effect of kaempferol and formononetin against myocardialoxidative stress damage. Liaoning J Tradit Chin Med. 2018;45:2465–68.
[48] Ibarra M, Prez-VizcaínoF, Cogolludo A, et al. Cardiovascular effects of isorhamnetin and quercetin in isolated rat and porcine vascular smooth muscle and isolated rat atria. Planta Med. 2002;68:307–10.
[49] Hubbard GP, Wolffram S, Vos R. de, et al. Ingestion of onion soup high in quercetin inhibits platelet aggregation and essential components of the collagen-stimulated platelet activation pathway in man: a pilot study. Br J Nutr. 2006;96:482–8.
[50] Pan JY, Jin ZG, Wu FH. Research advances in semen lepidii seu descurainiae and its formulae for cardiovascular diseases. J Tradit Chin Med. 2008;42:83–5.
[51] Wu J, Xiang JY, Sun YJ, et al. Molecular mechanism of aconiti lateralis radix praeparata-zingiberis Rhizoma against myocardial ischemia injury based on network pharmacology. Centr South Pharmacy. 2019;17:481–8.
[52] K. H. Wu, Sutdies on the Chemical Constituents and Bioactivities of Aconiti Lateralis Radix Praeparata. Beijing, China: China Academy of Chinese Medical Science. 2013.
[53] Yuan W. A research on the pharmacological action of fuzi. Clin J Chin Med. 2018;10:145–7.
[54] Matsui T, Li L, Wu JC, et al. Phenotypic spectrum caused by transgenic overexpression of activated akt in the heart. J Biol Chem. 2002;277:22896–901.
[55] Reinartz M, Raupach A, Kaisers W, et al. AKT1 and AKT2 induce distinct phosphorylation patterns in HL-1 Cardiac Myocytes. J Proteome Res. 2014;13:4232–45.
[56] DeBosch B, Sambandam N, Weinheimer C, et al. Akt2 regulates cardiac metabolism and cardiomyocyte survival. J Biol Chem. 2006;281:32841–51.
[57] Hers IVincent EE, Tavaré JM. Akt signalling in health and disease. Cell Signal. 2011;23:1515–27.
[58] Shioi T, McMullen JR, Kang PM, et al. Akt/protein kinase b promotes organ growth in transgenic mice. Mol Cell Biol. 2002;22:2799–809.
[59] Chang Z, Zhang Q, Feng Q, et al. Deletion of Akt1 causes heart defects and abnormal cardiomyocyte proliferation. Dev Biol. 2010;247:384–91.
[60] DeBosch B, Treskov L, Lupu TS, et al. Akt1 is required for physiological cardiac growth. Circulation. 2006;113:2097–104.
[61] Zeng Y, Du WW, Wu Y, et al. A circular RNA binds to and activates AKT phosphorylation and nuclear localization reducing apoptosis and enhancing cardiac repair. Theranostics. 2017;7:3842–55.
[62] Chan YY, Chang CS, Chien LH, et al. Apoptotic effects of a high performance liquid chromatography (HPLC) fraction of antrodia camphorata mycelia are mediated by down-regulation of the expressions of four tumor-related genes in human non-small cell lung carcinoma A549 cell. J Ethnopharmacol. 2010;127:652–61.
[63] Pollard TD, Earnshaw WC, Lippincott-Schwartz J, et al, Chapter 46: Programmed cell death. Cell Biology. 3rd edn. Elsevier lnc; 2017;797–815.
[64] Xue YT, Jiao HC, Lin X, et al. Effects of fuxin decoction on myocardial apoptosis signal transduction molecule Bcl-2 expression of heart failure rats. Chin Archives of Tradit Chin Med. 2013;31:2717–20+2876.
[65] Zhang LH, Wu JR, Jiang D, et al. Mechanism of 'paeoniae radix alba-cinnamomi ramulus' in the treatment of rheumatoid arthritis based on network pharmacology. Evaluation Analysis Drug-Use Hosp Chin. 2019;19:1057–64.
[66] Yun YT, Wang Y, Gong F. MAPK Signaling pathway regulates cardiomyocyte apoptosis in mice with post-infarction heart failure via endoplasmic reticulum stress response. Genomics Appl Biol. 2017;36:3438–46.
[67] Kanehisa M, Goto S. KEGG: kyoto encyclopedia of genes and genomes. Nucleic Acids Res. 2000;28:27–30.
[68] Zhao QF, Li HR, Chang LP, et al. Qiliqiangxin attenuates oxidative stress-induced mitochondrion-dependent apoptosis in cardiomyocytes via PI3K/AKT/GSK3β signaling pathway. Biol Pharm Bull. 2019;42:1310–21.
[69] Hegab Z, Gibbons S, Ludwig Neyses L, et al. Role of advanced glycation end products in cardiovascular disease. World J Cardiol. 2012;4:90–102.
[70] Chiang CE, Wang KL, Cheng HM, et al. Second revolution in cardiovascular prevention. J Chin Med Assoc. 2020;83:327–36.
[71] O'Meara E, McDonald M, Chan M, et al. CCS/CHFS heart failure guidelines: clinical trial update on functional mitral regurgitation, SGLT2 inhibitors, ARNI in HFpEF, and tafamidis in amyloidosis. Can J Cardiol. 2020;36:159–69.
[72] Nigro P, Abe J, Berk BC. Flow shear stress and atherosclerosis: a matter of site specificity. Antioxid Redox Signal. 2011;15:1405–14.
[73] Heusch G, Libby P, Gersh B, et al. Cardiovascular remodelling in coronary artery disease and heart failure. Lancet. 2014;383:1933–43.
[74] Hanahan D, Weinberg RA. Hallmarks of cancer: the next generation. Cell. 2011;144:646–74.
[75] Xue YT, Lin X, Gao Y, et al. Effect of fuxin decoction on TNF-α and BNP in myocardium of rats with heart failure. Chin J Integr Med Cardio-Cerebrovascular Disease. 2013;11:833–4.